An In-Plane Solid-Liquid-Solid Growth Mode for Self-Avoiding Lateral Silicon Nanowires

Linwei Yu,[1] Pierre-Jean Alet,[1,2] Gennaro Picardi,[1] and Pere Roca i Cabarrocas[1]

[1]*Laboratoire de Physique des Interfaces et des Couches Minces (LPICM), École Polytechnique, CNRS, 91128 Palaiseau, France*
[2]*CEA, DSM, IRAMIS, SPCSI, Laboratoire de chimie des surfaces et interfaces (LCSI), Centre de Saclay, 91191 Gif-sur-Yvette cedex, France*

(Received 11 October 2008; published 23 March 2009)

We report an in-plane solid-liquid-solid (IPSLS) mode for obtaining self-avoiding lateral silicon nanowires (SiNW) in a reacting-gas-free annealing process, where the growth of SiNWs is guided by liquid indium drops that transform the surrounding *a*-Si:H matrix into crystalline SiNWs. The SiNWs can be ~mm long, with the smallest diameter down to ~22 nm. A high growth rate of $>10^2$ nm/s and rich evolution dynamics are revealed in a real-time *in situ* scanning electron microscopy observation. A qualitative growth model is proposed to account for the major features of this IPSLS SiNW growth mode.

DOI: 10.1103/PhysRevLett.102.125501 PACS numbers: 81.07.Vb, 61.46.Km, 62.23.Hj, 81.16.Dn

One dimensional (1D) semiconductor nanowire structures, with novel electronic, optical, and thermal properties [1,2], are key functional elements for promising applications like nanowire transistors [3], biosensors [4], light emitting [5] and energy harvesting units [6,7]. Si nanowires (SiNW), compatible with the established Si technology, can be obtained in vertical arrays or bundles via various growth mechanisms like the vapor-liquid-solid (VLS) [8], the solution-liquid-solid [9], the oxide-assisted-growth [10], and the nickel-catalyzed solid-liquid-solid SiNW [11].

The electrical accessibility to SiNWs is one of the most critical issues for SiNW-based device applications [3,4], and in this respect the assembling and connection of SiNWs to predefined electrodes is a formidable challenge for large-scale integration of SiNW-based devices. Basically, the main difficulty in large-scale integration of SiNW-based devices is the incompatibility between the 3D VLS growth mode of SiNWs and the 2D planar device architecture, which necessitates an extra rearrangement or manipulation step to integrate vertical SiNWs into a 2D layout. From this point of view, a well-controlled in-plane growth of lateral SiNWs with natural connections to predesigned electrodes could represent an ultimate solution to a planar-architecture-compatible SiNWs-based device integration.

We have discovered an in-plane solid-liquid-solid (IPSLS) growth mode for such lateral SiNWs, where a liquid catalytic indium drop leads their in-plane growth by consuming and transforming surrounding *a*-Si:H into crystalline SiNW. Indium drops were first formed by a H_2 plasma treatment on top of a ITO substrate, [12] and then covered by a thin *a*-Si:H layer. The growth of lateral SiNWs is activated and sustained in a reactive-gas-free low temperature thermal annealing process. All this process is realized *in situ*, which avoids the potential oxidation or contamination. The rich growth dynamics of this IPSLS mode SiNW is revealed in a real-time *in situ* scanning electron microscopy (SEM) observation.

As shown in Figs. 1(a)–1(d), the ITO layer on Corning glass was firstly treated by using H_2 plasma in a plasma enhanced chemical vapor deposition (PECVD) system to form indium drops on the surface. The typical values for substrate temperature, treatment time, flow rate, chamber pressure and rf power density are 300 °C, 5–10 min, 100 sccm, 600 mTorr, and ~53 mW/cm^2, respectively. Then, the substrate with indium drops on top was covered by a layer of hydrogenated amorphous silicon (*a*-Si:H, 15–60 nm) deposited at 100–200 °C. Finally, the sample was annealed in vacuum ($\sim 10^{-6}$ mbar) at a temperature ranging between 300–500 °C for activating the growth of lateral SiNWs.

Figure 2(a) shows a typical SEM (Hitachi S4800) image of the as-grown lateral SiNWs after thermal annealing at 400 °C for 15 h, where the indium drops (the bright spots at the end of the SiNWs) lead the growth of the lateral SiNWs, with typical length of around ~20 μm. A close side view of a specific SiNW, as presented in Fig. 2(b), reveals that the SiNW, with a height of 3–4 times the *a*-Si:H thickness, *sits* in a wider ''trench'', which is formed by the catalyst drop. The self-avoiding phenomenon as witnessed in Fig. 2(a) can be understood as a consequence of the *a*-Si:H in the trench region being completely absorbed (or greatly thinned) by the catalyst drop. This interrupts the continuous supply of *a*-Si:H for the growth of SiNW and thus prevents the crossing of lateral SiNWs. According to the dimensions indicated in Fig. 2(b), the cross sectional area of the produced SiNW is roughly 85% of that of the trench, which could be due to (i) the volume contraction between amorphous and crystalline silicon, $\alpha \equiv V_c/V_a$, [13] and (ii) the loss of hydrogen from the *a*-Si:H film (which is ~10% at. in our case) during the transformation. The smallest IPSLS SiNWs observed so far in our experiment are ~22 nm in diameter, as shown in Fig. 2(c), while lengths up to 1 mm have been achieved.

The crystallinity of the lateral SiNWs was confirmed by using a confocal back-scattering Raman setup (Labram HR800 from Horiba Jobin-Yvon) with 633 nm laser exci-

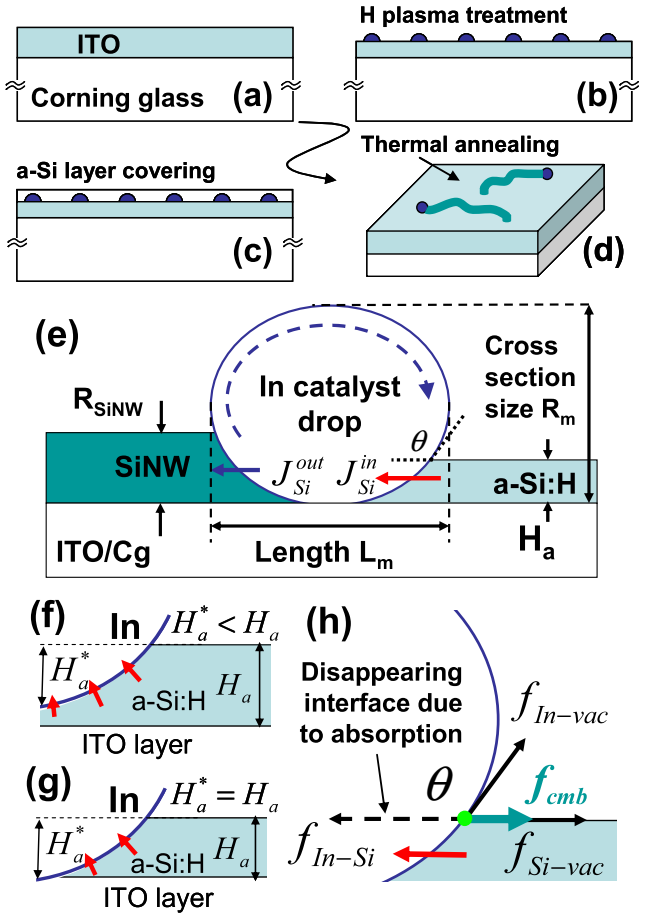

FIG. 1 (color online). (a)–(d) the basic experimental procedure for the growth of IPSLS SiNWs; (e) illustrates the IPSLS growth mode of SiNW, with J_{Si}^{out} (J_{Si}^{in}), R_m, L_m, R_{SiNW} and H_a, the flux of Si atoms from In drop to SiNW (from a-Si:H into In drop), the cross section and length of the In catalyst drop, the cross section of SiNW and the thickness of a-Si:H layer, respectively. (f) and (g) depict two possible situations for the actual absorbed a-Si:H thickness (H_a^*). (h) illustrates the origin of the drawing force at the imbalanced triple phase line due to continuous absorption at the In/a-Si:H interface.

tation (incident at 70°) optically coupled to an atomic force microscope (AFM, XE-100 PSIA). A contact mode AFM image of a SiNW segment is shown in Fig. 3(a), with the corresponding Raman signal intensity mapping on the same region in Fig. 3(b). Pixel color represents the intensity of the Raman signal integrated in the range $521 \pm 5\ \mathrm{cm}^{-1}$, the central position corresponding to the c-Si first order phonon band. As shown, the contour of the Raman mapping in Fig. 3(b), which is a convolution of the laser spot size ($\sim 2\ \mu$m) and the real morphology of SiNW, coincides well with the shape of the SiNW.

This *reacting-gas-free* IPSLS growth mode enables a real-time *in situ* observation of the growth of SiNWs in a SEM system (FEI Quanta 600F) equipped with a heating stage. The H_2 plasma treatment and a-Si:H covering processes were first done in a PECVD system, and then the sample was transferred to a heating stage in the SEM chamber for real-time characterization. Figures 4(a)–4(f) show a series of six frames captured in sequential order from a real-time observation of a SiNW, which is activated by thermal annealing at ~500 °C and guided by a *running* indium drop that keeps absorbing and transforming the a-Si:H matrix into crystalline SiNW behind. A close scrutiny of the frame series reveals a rich growth dynamics, which arises from the interplay between the front In/a-Si:H interface (at speed v_{ma}) and the rear SiNW/In interface (at speed v_{cm}). Specifically, the SiNW/In interface is found to be moving slightly faster than the In/a-Si:H interface ($v_{cm} > v_{ma}$), which leads to a two-step response of the liquid catalyst drop: first, the drop is gradually squeezed by the faster-moving SiNW from

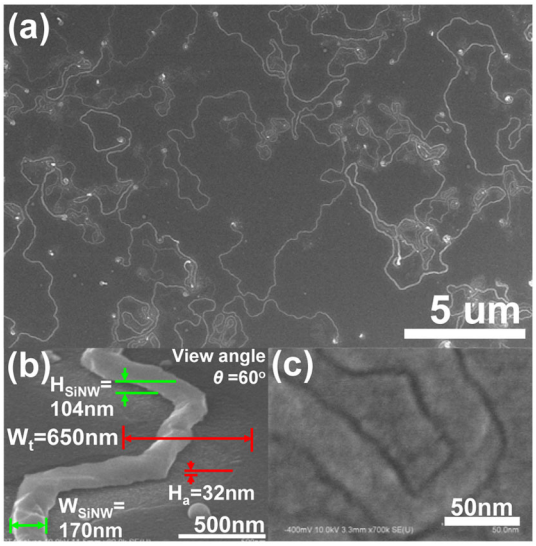

FIG. 2 (color online). (a) A typical SEM image of the lateral SiNWs, (b) a side-view of a SiNW sitting in a trench structure in the a-Si:H matrix, and (c) one of the smallest lateral SiNWs.

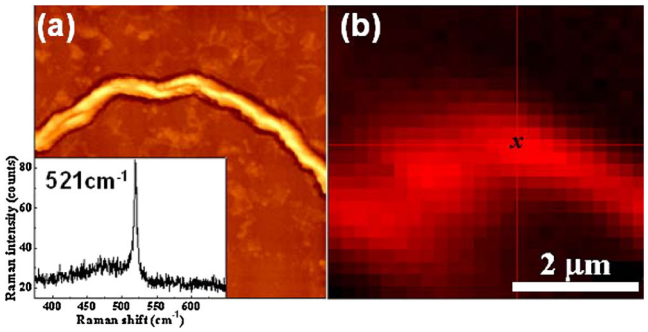

FIG. 3 (color online). (a) AFM image of a single SiNW with vertical scale from black to white of 160 nm, and (b) its corresponding crystalline Si Raman peak signal mapping (integrated in the spectral window $521 \pm 5\ \mathrm{cm}^{-1}$). The inset in (a) shows the Raman spectrum recorded from the position marked with an ***x*** in (b).

behind and deforms into a half spherical shape [Figs. 4(a)–4(d)]; then, it comes to a rapid change of moving direction and restores a spherical shape [Fig. 4(e)]. The details of the quick *restoration* process seem to be driven by the surface tension of the liquid drop to restore a more energetically favorable shape. This dynamic process repeats periodically during the growth to counteract the speed mismatch of the two interfaces and produces a bending trajectory of the as-produced SiNW [Fig. 4(f)]. According to the experimental observation, the diameter of the SiNWs R_{SiNW} is roughly proportional to the lateral cross section size of the catalyst drops R_m, with $f \equiv R_{\mathrm{SiNW}}^2/R_m^2 \approx 0.045 \pm 0.015$ being determined by the contact angle between SiNW and catalyst. Note that this periodic deformation/restoration of the catalyst drop also causes the surface corrugations on the SiNWs surface and trench sides.

The opposite case of $v_{\mathrm{cm}} < v_{\mathrm{ma}}$ is also observed, where the catalyst drop is found to be stretched. In this case, straighter SiNWs are produced, as shown, for example, by SiNW_C in Fig. 5. We note that this pulling force can be large enough to even break the SiNW as witnessed in real-time SEM observations (not shown here), indicating that an *independent* drawing force exists on the front catalyst/a-Si:H interface, with its speed v_{ma} solely related to the absorption rate of Si atoms from the a-Si:H matrix into indium catalyst.

Before a more detailed discussion of the dynamic behavior, it is interesting to make a comparison with the well-known VLS process. Similarly, the growth of IPSLS SiNW also consists of three steps: (i) the Si atoms are absorbed from the a-Si:H matrix at the front interface; then, (ii) the Si atoms diffuse across the catalyst drop and (iii) deposit at the SiNW/In interface. From an energetic point of view, the major driving force comes from the Gibbs energy difference between the crystalline and amorphous Si phases, which is about $\Delta E_{\mathrm{Si}} = E_{\mathrm{Si}}^a - E_{\mathrm{Si}}^c = 0.12$–$0.15$ eV/atom [14,15]. In contrast to the VLS mode where the growth is basically "friction-free", the catalyst drop in IPSLS mode has to overcome an *extra friction* between the liquid drop and the solid substrate. Nevertheless, the typical growth rate observed here, according to Figs. 4(a)–4(d) and 4(f), is as high as $v = 1.2 \times 10^2$ nm/s at 500 °C, which is almost 2 orders of magnitude higher than the highest growth rate of 3–4 nm/s (at 600 °C) achieved in our previous study of the In-catalyzed vertical VLS SiNWs. This much higher growth rate in the IPSLS mode can be related to the fact that the catalyst drop in IPSLS mode is in direct contact with a solid state a-Si:H precursor, with a 10^6–10^7 higher density than that achievable in gas phase. This guarantees a high influx rate of Si atoms ($J_{\mathrm{Si}}^{\mathrm{in}}$) into the catalyst. Moreover, the absorption of Si atoms from the a-Si:H matrix involves only the "Si-Si" bond breaking that is energetically less demanding than the "Si-H" bond breaking (silane decomposition) at the catalyst surface in VLS mode.

Note that the a-Si:H layer in the trench region could be completely or partially consumed by the catalyst drop, as indicated in Figs. 1(e) and 1(f), which corresponds to the cases of $H_a^* = H_a$ or $H_a^* < H_a$, with H_a^* and H_a being the actual absorbed and total thickness of the a-Si:H layer, respectively. These two situations can be clearly distinguished from the different contrasts and surface features of the reexposed ITO or the residual a-Si:H, as shown, for example, by the SiNW_A and SiNW_B in Fig. 5, respectively. The existence of residual a-Si:H in the trench region suggests that (i) saturation concentration (with respect to the a-Si/In interface) has been reached in the catalyst, or (ii) the catalyst is moving too quickly to fully absorb the underlying a-Si:H.

The typical time scale for the Si atoms diffusing through an indium drop of $L_m = 200$–500 nm is $t_d \approx L_m^2/D_{\mathrm{Si}} = 0.02$–$0.1$ ms (at 400 °C), with $D_{\mathrm{Si}} \approx 2 \times 10^{-9}$ m^2/s the binary diffusion coefficient of Si atom in indium [16]. To sustain a growth rate of $v \approx 10^2$ nm/s (equivalent to a Si atom flux of $J_{\mathrm{SiNW}} = v/\Omega_{\mathrm{Si}}$, with Ω_{Si} the atom volume of Si), the concentration gradient ΔC_{Si} across a catalyst drop of 500 nm (for driving a Si atom flux of

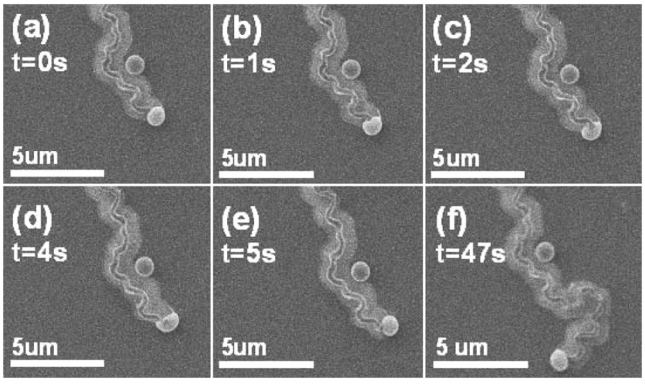

FIG. 4. (a)–(f) a series of six frames captured in sequential order (with $t = 0$, 1, 2, 4, 5, 47 s) in a real-time *in situ* SEM observation. A gradual squeezing of the In drop by the SiNW behind can be clearly witnessed in (a)–(d), followed by a quick restoration (d)–(e).

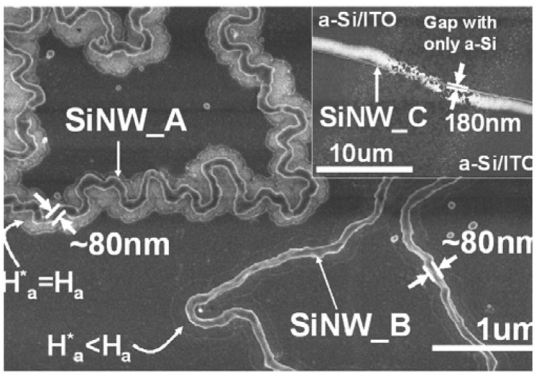

FIG. 5. shows three SiNWs (A, B, and C) obtained on the same sample but with different morphologies.

$J_{\mathrm{Si}} = D_{\mathrm{Si}}\Delta C_{\mathrm{Si}}/L_m$) can be estimated, with the continuity condition at the SiNW/In interface $J_{\mathrm{SiNW}}R^2_{\mathrm{SiNW}} = J_{\mathrm{Si}}R^2_m$, to be

$$\Delta C_{\mathrm{Si}} = vL_m f/(D_{\mathrm{Si}}\Omega_{\mathrm{Si}}) \approx 10^{16}\ \mathrm{at./cm^3}, \qquad (1)$$

which, according to the solubility of Si in In [17], accounts for only ~2% (~0.3%) of the equilibrium Si concentration $C^c_{\mathrm{eq}} = 3\times10^{18}$ at./cm^3 at 400 °C (2×10^{19} at/cm^3 at 500 °C) at the c-Si/In interface. So, the diffusion mass transport is still a quick process.

The speeds of the front In/a-Si : H interface (v_{cm}) and the rear SiNW/In interface (v_{ma}) are related to the absorption flux from a-Si:H ($J_{a\text{-Si}}$) and the deposition flux onto SiNW (J_{SiNW}), respectively. In a balanced condition, one obtains

$$S_{\mathrm{SiNW}}v_{\mathrm{cm}} \approx \alpha R_m H^*_a v_{\mathrm{ma}}, \qquad (2)$$

with $S_{\mathrm{SiNW}} = R^2_{\mathrm{SiNW}} = fR^2_m$ being the cross section area of SiNW. Thus, the relative speed of the two moving interfaces can be defined as

$$\eta \equiv v_{\mathrm{cm}}/v_{\mathrm{ma}} \approx \frac{\alpha H^*_a}{R_m f} = AH^*_a/R_{\mathrm{SiNW}}, \quad \text{with} \quad A = \alpha f^{-1/2}. \qquad (3)$$

As can be seen, the relative speed ratio η is proportional to H^*_a/R_{SiNW}. In principle, for $\eta > 1$ ($v_{\mathrm{cm}} > v_{\mathrm{ma}}$), the growing SiNW pushes the catalyst drop from behind and squeezes it, causing the swaying response of catalyst drop and producing relatively bending SiNWs, as shown in Fig. 4; On the contrary for $\eta < 1$ ($v_{\mathrm{cm}} < v_{\mathrm{ma}}$), the growing SiNW always lags behind and is stretched by the catalyst drop, resulting a straighter SiNW (for example, the almost perfect straight SiNW_C in Fig. 5).

To provide a qualitative test of the influence of η, let us examine the three SiNWs (A, B and C) shown in Fig. 5, and compare their different absorbed a-Si:H thickness H^*_a and size R_{SiNW}. We can see that $H^*_{a\_A} = H^*_{a\_C} > H^*_{a\_B}$ (since the a-Si:H in the trench of SiNW_B is only partially consumed) and $R^A_{\mathrm{SiNW}} \approx R^B_{\mathrm{SiNW}} \approx 80\,\mathrm{nm} < R^C_{\mathrm{SiNW}} \approx 180\,\mathrm{nm}$, as indicated in Fig. 5. According to the ratio $\eta \sim H^*_a/R_{\mathrm{SiNW}}$, the SiNW trajectory can be changed by either reducing H^*_a or by increasing R_{SiNW}. The first case is justified by the straighter trajectory of the SiNW_B, with $H^*_{a\_B} < H^*_{a\_A}$ with $R^B_{\mathrm{SiNW}} \approx R^A_{\mathrm{SiNW}}$ and thus $\eta_B < \eta_A$; The second assumption is also supported by comparing SiNWs A and C. Indeed, we see that SiNW_C, with $H^*_{a\_C} = H^*_{a\_A} = H_a$ and $R^C_{\mathrm{SiNW}} > R^A_{\mathrm{SiNW}}$ and thus $\eta_C < \eta_A$, is almost perfect straight. We suggest that this simple but useful relation indicates an effective way to tune the morphology (and even the strain state) of the IPSLS SiNWs.

We propose that the drawing force on the front catalyst/a-Si:H interface results from the imbalanced triple phase line. As illustrated in Fig. 1(h), during the growth of SiNWs, the catalyst/a-Si:H interface (immersed in the catalyst) is continuously weakened as Si atoms are absorbed into the indium catalyst. As a consequence, the balance in the *horizontal direction* between the surface/interface tensions, In/vacuum (f_{In}), a-Si:H/vacuum ($f_{a\mathrm{Si}}$) and In/a-Si:H ($f_{\mathrm{In}\text{-}a\mathrm{Si}}$), which in case of no absorption should be $f_{\mathrm{In}\text{-}a\mathrm{Si}} = f_{a\mathrm{Si}} + f_{\mathrm{In}}\cos\theta$, is broken due to the "disappearing" of $f_{\mathrm{In}\text{-}a\mathrm{Si}}$ interface tension. As a result, the triple-phase-line is drawn forward to form a new In/a-Si:H interface and to reestablish the balance, which however will soon be broken again due to the continuous absorption process. So, a *drawing force* will always be exerted on the triple-phase-line interface (given that the absorption is continuous). Moreover, since the bottom interface of the catalyst drop is subject to a larger friction than the top surface, it is possible that the liquid catalyst could be forced into a *rolling forward* movement, as indicated by the dashed blue line in Fig. 1(e).

In summary, we report an in-plane solid-liquid-solid (IPSLS) growth mode of lateral SiNW obtained in an all-*in situ* process. The growth of SiNW is promoted by indium catalyst drops which transform the surrounding a-Si:H matrix into crystalline SiNW. An ultrahigh growth rate (>10^2 nm/s) and rich growth dynamics are directly observed in a real-time *in situ* SEM observation. This IPSLS growth mode of SiNWs opens new opportunities for large-scale integration of SiNWs-based nanodevices.

The authors gratefully thank Daniel Caldemaison from Laboratoire de Mécanique des Solides (LMS) for his help with the real-time *in situ* SEM characterizations.

[1] L. Wei and M. L. Charles, J. Phys. D **39**, R387 (2006).
[2] C. M. Lieber, Mater. Res. Bull. **28**, 486 (2003).
[3] Y. Cui *et al.*, Nano Lett. **3**, 149 (2003).
[4] Y. Cui *et al.*, Science **293**, 1289 (2001).
[5] P. Ball, Nature (London) **409**, 974 (2001).
[6] B. Z. Tian *et al.*, Nature (London) **449**, 885 (2007).
[7] A. I. Hochbaum *et al.*, Nature (London) **451**, 163 (2008).
[8] R. S. Wagner and W. C. Ellis, Appl. Phys. Lett. **4**, 89 (1964).
[9] A. T. Heitsch *et al.*, J. Am. Chem. Soc. **130**, 5436 (2008).
[10] R.-Q. Zhang, Y. Lifshitz, and S. T. Lee, Adv. Mater. **15**, 635 (2003).
[11] L. Eun Kyung *et al.*, Nanotechnology **19**, 185701 (2008).
[12] P.-J. Alet *et al.*, J. Mater. Chem. **18**, 5187 (2008).
[13] O. Renner and J. Zemek, Czech. J. Phys. **23**, 1273 (1973).
[14] S. Roorda *et al.*, Phys. Rev. Lett. **62**, 1880 (1989).
[15] I. Stich, R. Car, and M. Parrinello, Phys. Rev. B **44**, 11 092 (1991).
[16] A. U. Coskun, Y. Yaman, and A. Faruk, Model. Simul. Mater. Sci. Eng. **10**, 539 (2002).
[17] C. D. Thurmond, J. Phys. Chem. **57**, 827 (1953).